Global Change Biology (2000) **6,** 227–245

The high-latitude terrestrial carbon sink: a model analysis

A. WHITE, M. G. R. CANNELL and A. D. FRIEND
Institute of Terrestrial Ecology, Bush Estate, Penicuik, Midlothian, EH26 0QB, UK

Abstract

A dynamic, global vegetation model, hybrid v4.1 (Friend *et al*. 1997), was driven by transient climate output from the UK Hadley Centre GCM (HadCM2) with the IS92a scenario of increasing atmospheric CO_2 equivalent, sulphate aerosols and predicted patterns of atmospheric N deposition. Changes in areas of vegetation types and carbon storage in biomass and soils were predicted for areas north of 50°N from 1860 to 2100. Hybrid is a combined biogeochemical, biophysical and biogeographical model of natural, potential ecosystems. The effect of periodic boreal forest fires was assessed by adding a simple stochastic fire model. Hybrid represents plant physiological and soil processes regulating the carbon, water and N cycles and competition between individuals of parameterized generalized plant types. The latter were combined to represent tundra, temperate grassland, temperate/mixed forest and coniferous forest. The model simulated the current areas and estimated carbon stocks in the four vegetation types.

It was predicted that land areas above 50°N (about 23% of the vegetated global land area) are currently accumulating about 0.4 PgC y^{-1} (about 30% of the estimated global terrestrial sink) and that this sink could grow to 0.8–1.0 PgC y^{-1} by the second half of the next century and persist undiminished until 2100. This sink was due mainly to an increase in forest productivity and biomass in response to increasing atmospheric CO_2, temperature and N deposition, and includes an estimate of the effect of boreal forest fire, which was estimated to diminish the sink approximately by the amount of carbon emitted to the atmosphere during fires. Averaged over the region, N deposition contributed about 18% to the sink by the 2080 s. As expected, climate change (temperature, precipitation, solar radiation and saturation pressure deficit) and N deposition without increasing atmospheric CO_2 produced a carbon source. Forest areas expanded both south and north, halving the current tundra area by 2100. This expansion contributed about 30% to the sink by the 2090 s. Tundra areas which were not invaded by forest fluctuated from sink to source. It was concluded that a high latitude carbon sink exists at present and, even assuming little effect of N deposition, no forest expansion and continued boreal forest fires, the sink is likely to persist at its current level for a century.

Keywords: carbon sink, climate change, elevated CO_2, nitrogen, tundra, fire, boreal forest

Received 9 May 1999; resubmitted and accepted 8 July 1999

Introduction

A carbon sink of about 1.6 Pg y^{-1} is required to balance the current global carbon budget (Houghton *et al*. 1998). It is necessary to know the processes which determine the magnitude and whereabouts of this sink in order to forecast how it may operate as climate and land use change in the future. A level of climate change which caused a disappearance or reversal of the terrestrial carbon sink would, of itself, constitute a dangerous climate change in the terms of Article 2 of the UN Framework Convention of Climate Change (Parry *et al*. 1996; White *et al*. 1997; Cao & Woodward 1998a,b). Northern high latitudes may be particularly important,

Correspondence: A. White, Department of Mathematics, Heriot-Watt University, Edinburgh EH14 4AS, fax +44 131 451 3249, e-mail a.r.white@ma.hw.ac.uk

because of their large land area and carbon pool size, the large increase in temperature and regionally large increases in N deposition they are forecast to experience, and the potential for climate-driven shifts in biome distribution. This study therefore focused on processes regulating the current and future operation of the carbon sink in this region, defined as the land area north of 50°N.

There is considerable evidence that northern terrestrial ecosystems may currently be a carbon sink. First, there is evidence from analyses of the global CO_2 flask network (Conway *et al*. 1994), isotope tracers and both forward and inverse modelling of atmospheric CO_2 concentrations (abbreviated as [CO_2]) (Ciais *et al*. 1995; Denning *et al*. 1995; Enting *et al*. 1995) and the increasing seasonal amplitude of [CO_2] at northern latitudes (Keeling *et al*. 1996; Randerson *et al*. 1997). Secondly, there is evidence that many forests are growing faster than hitherto, from analyses of growth data across Europe (Spiecker *et al*. 1996), tree ring patterns averaged over northern regions and near the tree-line (Briffa *et al*. 1998; Rolland *et al*. 1998), satellite and ground observations of growing season length (Goulden *et al*. 1996; Myneni *et al*. 1997) and forest inventories, which combine land use and climate effects (Dixon *et al*. 1994; Houghton 1996).

There is, however, a recent analysis suggesting that the northern sink is below the 50°N parallel (Fan *et al*. 1998) and there are observations that the Arctic tundra may have become a carbon source of about 0.19 PgC y^{-1} in response to soil warming and drying in recent years (Oechel & Vourlitis 1994; Oechel *et al*. 1993). However, measurements made over a few years may not reflect the long-term trend, because the balance between soil respiration and net primary production (NPP) in this region may alternate from positive to negative depending on the degree of soil drying (McKane *et al*. 1997). Over periods of a few years, there seem to be positive time-lagged correlations between changes in [CO_2] and temperature at northern latitudes, suggesting that warm years create a carbon source and cool years a sink (Keeling *et al*. 1995; Braswell *et al*. 1997). Averaged over the region, and in the longer term, it is unclear whether the tundra will be a carbon sink, source or carbon neutral.

The future carbon balance at high latitudes in response to climate change depends on the balance between (i) processes which alter heterotrophic respiration, particularly the warming of organically rich soils (e.g. Gorham 1991; Goulden *et al*. 1998), drying of wetlands (McKane *et al*. 1997) and lags between forest dieback and expansion (Smith & Shugart 1993), and (ii) processes which alter the net primary productivity of vegetation (NPP, which at equilibrium equals the total litter input to the soil) through changes in plant physiological processes and areas of different types of vegetation. With such a complex system, it is not surprising that ecosystem models give predictions ranging from a substantial high latitude carbon sink (e.g. King *et al*. 1997; Cao & Woodward 1998a,b; Xiao *et al*. 1998) a small sink (Kohlmaier *et al*. 1995) to a source (Wang & Polglase 1995).

Clearly, uncertainties in the structure and parameterization of complex ecosystem models mean that they can never predict the future with certainty, any more than GCMs can (Hurtt *et al*. 1998). However, models are becoming more believable as they meet some essential criteria. It is only within the last decade that 'dynamic global vegetation models' (DGVMs) have begun to combine (i) coupled plant-soil carbon, N and water (biogeochemical) cycles (ii) atmosphere–vegetation energy and mass (biophysical) fluxes, and (iii) dynamic (biogeographical) shifts in vegetation types and properties (Neilson & Running 1996; Hurtt *et al*. 1998; Neilson *et al*. 1998). Also, it is only within the last few years that transient GCM climate predictions have become available and have been shown to produce very different vegetation responses from equilibrium climates (e.g. Xiao *et al*. 1998; Foley *et al*. 1996; Neilson & Draper 1998) and consideration has been given to spatial patterns of atmospheric N deposition (Hudson *et al*. 1994; Townsend *et al*. 1996; Holland *et al*. 1997).

This study offers an advance by using a DGVM (hybrid v4.1) which combines biogeochemical, biophysical and biogeographical processes, simulates annual competition between plant types as they grow, evaluates the impact of periodic fires and is driven by both transient GCM output and predicted patterns of N deposition. The magnitude of the high-latitude carbon sink may still be uncertain, because it depends on model parameterization, but the nature of this model and simulations give increased confidence in its predictions on the relative roles of different ecosystem types, vegetation transition, warming, elevated CO_2 and N deposition.

Overview of the dynamic global vegetation model, hybrid v4.1

A complete description of the hybrid model is given by Friend *et al*. (1997) and Friend & White (1999). The model has been evaluated for its ability to simulate current measured carbon fluxes at particular sites (Friend *et al*. 1997) and it has been shown to successfully predict the major global patterns of undisturbed preindustrial vegetation, NPP, biomass and soil carbon (Friend & White 1999). Here, we outline the essential properties of the model and modifications that were made for this study.

Table 1 Vegetation types defined in this study, showing their relationship to eight generalized plant types in hybrid v4.1 (defined by C3 or C4 photosynthesis and phenology) and three main classes (defined by the parameters given in Table 2)

Main classes	Herbaceous	Broadleaved tree	Needleleaved tree
Generalized plant types	1) [C4 photosythesis][1] 2) C3 photosynthesis	3) [Evergreen][2] 4) Cold deciduous 5) Dry deciduous	6) [Dry deciduous][2] 7) Cold deciduous 8) Evergreen
Vegetation types defined in this study	**Tundra**: i) regions north of 60°N ii) herbaceous biomass >10% of total tree biomass **Temperate grassland**: i) regions between 50° and 60°N ii) herbaceous biomass >10% of total tree biomass	**Temperate/mixed forest**: 90–100% of biomass is (4) or (5) mixed with (7) or (8)	***Coniferous forest:*** 90–100% biomass is (7) or (8)

[1]This generalized plant type occurred rarely north of 50°N.
[2]These generalized plant types did not occur north of 50°N.

The model operates conceptually like a forest gap model, in which individuals of all potential plant types are seeded every year into 200 m^2 plots (with no dispersal constraint) grow, die and regenerate year by year, with all underlying processes calculated on a subdaily timestep. Vegetation types are assigned different parameter values which determine their success in competing for light, water and N in any climatic regime and hence the resulting vegetation. Thus, the model describes the transient responses and properties of vegetation, which can be composed of different proportions of specified plant types at any time. However, unlike most gap models, plant growth is determined entirely by climatic variables operating through plant physiological and soil processes. The carbon, water and nutrient cycles are coupled, including all the major interactions, feedbacks and exchanges between the soil, vegetation and atmosphere. The model contains no statistical relationships between vegetation properties and the current climate except for phenology.

The model, as described by Friend *et al*. (1997) and Friend & White (1999), does not include land-use change or disturbance due to fire, which is critically important in the boreal region. In this study, a simple stochastic fire model was incorporated into hybrid to estimate the effect of fire on carbon storage and fluxes in the boreal needleleaved forest (see below).

Plant and vegetation types

The model is parameterized for three **main classes** of vegetation; herbaceous, broadleaved trees and needleleaved trees, which are given different values of up to 16 parameters (Table 2, see below). These main classes are then divided into eight **generalized plant types**, as shown in Table 1, by distinguishing C3 and C4 herbaceous plants, evergreen and deciduous trees and cold and dry deciduous trees. C3 and C4 herbaceous plants have different photosynthesis submodels; cold deciduous trees shed their leaves in response to daylength and refoliate in response to a degree-day requirement; dry deciduous trees shed their leaves when the soil water potential falls below −1.49 MPa and refoliate when it rises above −0.5 MPa. North of 50°N, there were no dry deciduous needleleaved or evergreen broadleaved trees and C4 herbaceous plants (grasses) occurred only on the 50°N boundary in eastern Europe and central Asia.

In this study, the generalized plant types were grouped to produce four **vegetation types** based on the percentage biomass of each generalized plant type, as defined in Table 1. These vegetation types were: *tundra*, *temperate grassland*, *temperate/mixed forest* and *coniferous forest*, approximately corresponding to the vegetation types used by Matthews (1983) and Olson *et al*. (1983). The temperate grassland excluded large areas of steppe and prairie south of 50°N and the coniferous forest included the carbon rich peatlands and wetlands which occur on the northern boundary of the boreal forests.

Key processes represented

The canopy is divided into 1 m layers and attenuation down the canopy of photosynthetically active and short wave radiation is calculated using Beer's law with defined extinction and reflection coefficients (Table 2, parameters 1–4). Canopy photosynthesis is linearly related to the photosynthetic rate of the uppermost leaves. The vertical profile of N in the canopy is optimized to the time-mean profile of PAR.

Table 2 Parameters used to define the three main classes of plants in hybrid v4.1 (Friend *et al.* 1997)

Parameter	Herbaceous	Broadleaf tree	Needleleaf tree	Units
Shortwave irradiance extinction coefficient	0.48	0.48	0.48	dimensionless
Shortwave irradiance reflection coefficient	0.20	0.20	0.11	fraction
Photosynthetically active irradiance extinction coefficient	0.65	0.65	0.50	dimensionless
Photosynthetically active irradiance reflection coefficient	0.05	0.05	0.03	fraction
Fraction of foliage N not used in Rubisco or thylakoids	0.67	0.67	0.83	fraction
Ratio between max. stomatal conductance and Rubisco N	1359	1670	2220	mol(H_2O) $m^{-2}s^{-1}$/ (kg (RubiscoN) m^{-2})
Ratio of bark thickness to *D* (diameter)	–	0.033	0.03	m m^{-1}
Tree form factor (used for calculating woody carbon mass)	–	0.60	0.56	dimensionless
Allometry coefficient for *H* (height) from *D* (diameter)	–	28.51	32.95	m^{-1}
Allometry exponent for *H* (height) from *D* (diameter)	–	0.467	0.588	dimensionless
Fraction of wood plus bark below ground	–	0.220	0.222	fraction
Mean wood plus bark density	–	305	205	kg C m^{-3}
Maximum foliage to sapwood area ratio	–	4170	3330	m^2 m^{-2}
Fraction of sapwood alive	–	0.1700	0.0708	fraction
Specific leaf area	36	36	12	m^2 kg C^{-1}
Turnover rate of foliage	1.13	1.00	0.33	fraction y^{-1}

C3 and C4 photosynthesis are calculated using a biochemical approach based on Farquhar & von Caemmerer (1982) and Collatz *et al*. (1991), respectively. The three main classes differ in the fraction of foliage N not used in Rubisco or thylakoids (Table 2, parameter 5). Stomatal conductance is calculated using empirical relationships between stomatal conductance and irradiance, soil water potential, air temperature, above-canopy water vapour pressure deficit and above-canopy [CO_2] [Jarvis (1976) adapted by Stewart (1988) see also, Friend (1995)]. The main classes differ in the ratio between maximal stomatal conductance and Rubisco N (Table 2, parameter 6). Foliage and fine root maintenance respiration rates are linear functions of N content; sapwood maintenance respiration is a linear function of living sapwood biomass. Herbaceous respiration rates are linear functions of biomass. All respiration components are exponential functions of air temperature.

Trees are assigned initial diameters, which then determine the leaf area index and biomass of tree parts according to allometric relationships. Wood cross-sectional area at breast height is calculated assuming a ratio of d.b.h. to bark thickness (Table 2, parameter 7). Woody biomass is then calculated using a form factor (Table 2, parameter 8), calculated tree height (Table 2, parameter 9 and 10), a proportion of woody biomass below-ground (Table 2, parameter 11) and wood specific gravity (Table 2, parameter 12). There are also defined values for ratio of foliage to sapwood area, fraction of live sapwood, specific leaf area and turnover rate of foliage (Table 2, parameters 13–16).

N uptake is a function of fine root biomass, plant C:N ratio, soil surface temperature and soil mineral N, which includes N biologically fixed and deposited from the atmosphere. Trees have access to all mineral N, whereas the herbaceous layer has access to only a fraction, given by the ratio of the soil-water holding capacity of the top two hydrological layers over the total capacity for all three layers.

For trees, the maximum possible foliage and fine root C and N contents are calculated at the beginning of the year. During the year, litter C and N are lost from these components (different tree species are assumed to have the same fine root turnover but different foliage turnover rates, Table 2), and if sufficient storage is available they are restored to their maximum values. If the lowest 1 m of the crown experiences a negative C balance then the maximum foliage area in the next year is given by the amount of foliage displayed above the lowest layer and the height to the base of the crown is increased by 1 m. Also, since the foliage to sapwood area is fixed, when trees experience a negative C balance at the base of their crowns some sapwood will be converted to heartwood. A fixed ratio between foliage mass and fine root mass, and a fixed fraction of woody tissue below ground are also assumed.

For herbs and grasses, C and N litter production is calculated as a fixed fraction of the foliage, structural and fine root compartments. Allocation of C is parameterized to maintain fixed ratios between these compartments. If the lowest 10% of foliage has a net negative C balance on the previous day, then the new foliage area is limited to a maximum of 90% of its previous value. Any C remaining after allocation is added to a storage pool. N is allocated to maintain fixed relative C:N ratios between the three tissue compartments.

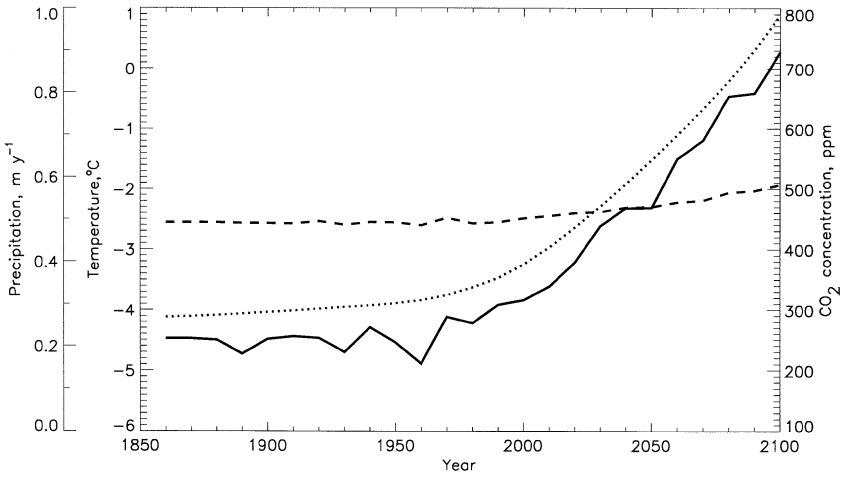

Fig. 1 Mean annual temperature (solid line) and precipitation (dashed line) predicted by the Hadley Centre GCM (HadCM2), averaged over the land area above 50°N, assuming an IS92a scenario of increasing atmospheric CO_2 concentration (dotted line). Large interannual variability has been smoothed by taking decadal means.

The daytime energy balance of the canopy is solved to calculate the rate of transpiration and foliage temperature. Interception loss is calculated. For this application the soil hydrology model was modified from that described by Friend *et al*. (1997). The soil C and N dynamics model is based on Century (Parton *et al*. 1993) as formulated by Comins & McMurtrie (1993). The soil is divided into three layers: 0–5 cm, 5–20 cm and 20–100 cm depth. Herbaceous vegetation has access to water and N in the top two layers, whereas trees can access all layers. The total soil water holding capacity is determined from soil carbon. A simple routine (a development of the method of Wang & Polglase 1995) is used to calculate the depth of frozen soil (previously, hybrid assumed all soil was frozen if the 24 h mean temperature was below zero), with all water below this depth assumed frozen, and therefore unavailable (see Appendix). The resistence to drainage is also increased if there is frozen soil in the top 1 m of soil.

Climate predictions, N deposition and model runs in the absence of fire

The hybrid model was driven by transient climate output from the UK Hadley Centre coupled atmosphere–ocean GCM (HadCM2), supplied as monthly means with predicted levels of interannual variability. The mean was taken of four runs of the GCM. Atmospheric CO_2 concentrations (including other greenhouse gas CO_2 equivalents) were increased according to the IPCC business-as-usual scenario 1992a (IS92a), from 280 ppm in 1860 to nearly 800 ppm in 2100 (Fig. 1). Sulphate aerosols were included. The GCM predictions closely matched the observed climate since preindustrial times (Mitchell *et al*. 1995; Johns *et al*. 1997). However, as with most GCMs, predicted climate anomalies were considered to be more reliable than the absolute climate predictions.

Consequently, GCM anomalies of temperature, diurnal temperature range, relative humidity, downward short-wave radiation and precipitation were calculated as mean decadal monthly differences relative to the 1970s. These anomalies were then added to a global observational climatology (Friend 1998) after this climatology had been re-gridded from the 0.5° latitude–longitude scale to that of the GCM (i.e. 2.5–3.75° latitude–longitude). Daily values of the climate variables, required by hybrid, were then derived using a stochastic weather generator parameterized for each decade using mean monthly values (Richardson & Wright 1984; Friend 1998).

Averaged over the region, mean annual temperatures were predicted to increase from about −4.7 °C to 0.3 °C between 1860 and 2100 (Fig. 1). Figure 2(a) shows the spatial distribution of 1860 mean annual temperatures. The warming predicted between the 1860s and 2090s varied from about 2 °C in areas close to the 50 °N parallel to 6–8 °C near the pole (Fig. 2b). Overall, precipitation increased from about 0.50 m y^{-1} in 1860–0.58 m y^{-1} in 2100 (Fig. 1), the largest increases occurred in central western Asia and Canada south of 60°N (Fig. 2c).

Biological N fixation was assumed to be 10 kg N ha^{-1} y^{-1}. Atmospheric N deposition for each grid cell was derived from NH_x and NO_y deposition estimates for preindustrial, current, and 2050 conditions (Holland *et al*. 1997; Dentener, pers. comm.), assuming an exponential increase with time. Regions north of 50°N currently account for 15% of global N deposition, decreasing to 12% by 2050. Most of this deposition occurs in central and western Europe, where the predicted increase in N deposition was commonly greater than 20 kg N ha^{-1} y^{-1} (Fig. 2d).

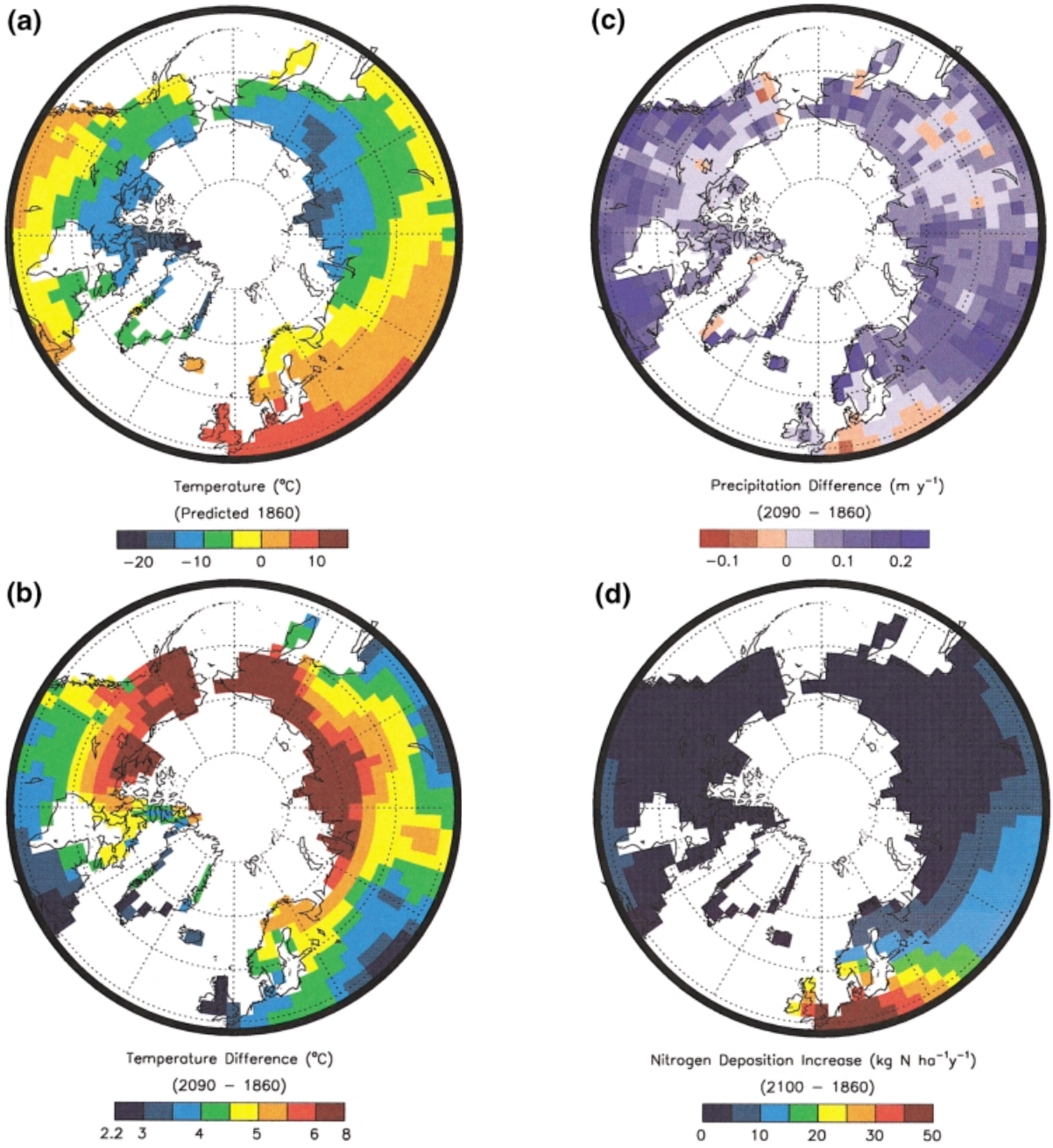

Fig. 2 Transient climate predictions from the Hadley Centre GCM (HadCM2) and increases in atmospheric N deposition from Holland *et al.* (1997). (a) mean annual temperature in 1860 (b) increase in mean annual temperature between the 1860s and 2090s (c) change in mean annual precipitation between the 1860s and 2090s, and (d) increase in annual N deposition between the 1860s and 2090s.

The model, hybrid, was 'spun up' for 500 years to reach a near steady-state in the 1860 climate. It was then run to 2100 in transient simulations with 10 independent 200 m^2 plots in each GCM grid square north of 50°N, with (a) both climate (temperature, rainfall, humidity and solar radiation) changing and [CO_2] increasing, and (b) climate changing but [CO_2] fixed at 280 ppm

Evaluation of the impact of fire in the boreal zone

Hybrid v4.1 has a tree mortality regime which kills an individual tree in the boreal region on average about every 400 years, creating a gap for regeneration. When this occurs, all the biomass carbon and nitrogen enters

Table 3 Predicted present day areas and carbon stocks of northern ecosystems predicted in this study and compared with estimates made by Post *et al*. (1982), Matthews (1983) and Olson *et al*. (1983). Vegetation carbon stocks are calculated as the product of the area given by Post *et al*. (1982) and the carbon per unit area estimated from Olson *et al*. (1983)

	Area ($\times 10^{12}$ m^2)		
Vegetation type	This study (> 50°N)	Matthews (1984) (> 50°N)	Post *et al*. (1982) Northern ecosystems
Tundra	7.9	7.6	8.8
Coniferous forest	14.3	13.9[1]	13.9[4]
Temperate/mixed forest	5.9	5.9[2]	3.4[5]
Temperate grassland	2.6	3.3[3]	[15.2][6]
	30.7	30.7	41.3

	Soil Carbon (Pg)		Vegetation Carbon (Pg)	
	This Study (> 50°N)	Post *et al*. (1982) Northern ecosystems	This Study (> 50°N)	Olson *et al*. (1983) Northern Ecosystems
Tundra	230	192	17	9
Coniferous forest	497	384[4]	65	61[4]
Temperate/mixed forest	117	43[5]	61	55[5]
Temperate grassland	26	[182][6]	12	10[6]
	870	801	155	135

[1], [2], and [3] are the following combination of vegetation classes from Matthews (1983) occurring north of 50°N. [4], [5], and [6] are the following combination of vegetation classes from Post *et al*. (1982).
[1]Temp/subpolar evergreen needleleaf forest, evergreen needleleaf woodland and cold deciduous woodland.
[2]Cold deciduous forest (with evergreens) and cold deciduous forest (without evergreens)
[3]All grassland classes and all shrub classes.
[4]Boreal forest (wet), boreal forest (moist) and peatlands/wetlands.
[5]Temperate forest cool
[6]Cool temperate steppe, boreal desert and cool desert.

the soil as litter. To represent fire, an additional routine was added which burned all vegetation within each 200 m^2 plot with a probability of 0.006, equivalent to a return period of 167 years (a reasonable historic average; Kurz & Apps 1995). All the carbon and nitrogen in the foliage and half that in the stems was lost to the atmosphere, the remainder entered the soil as litter.

Hybrid was run with and without this fire model for 100 plots within a grid square in southern Quebec, which was dominated by needle-leaved forest, with IS92a transient climate change and increasing CO_2 from 1860 to 2100.

Results

Predicted areas and carbon stocks in northern ecosystems in the absence of fire

The model predicted that the present-day area of *tundra* is about 7.9×10^{12} m^2 (million km^2), which corresponded closely with estimates made by Post *et al*. (1982) and Matthews (1983) (Table 3). The area of *coniferous forest* (including cold deciduous forest and all types of boreal evergreen forests, many growing in peatlands and wetlands) was predicted to be about 14.3×10^{12} m^2, also in agreement with observed estimates (Table 3). The area defined as *temperate/mixed forest* was estimated to be about 5.9×10^{12} m^2, similar to Matthews (1983) but greater than the area of 'cool temperate' forest defined by Post *et al*. (1982) (Table 3). The area defined here as *temperate grassland* was only about 2.6×10^{12} m^2, being limited to the areas between 50 and 60°N which has a low woody biomass.

The present-day carbon stocks which were generated by the model totalled about 1025 Pg, 85% of which was in the soil (Table 3). Over half of the 870 Pg of soil carbon was predicted to occur in coniferous forest soils, including peatlands and wetlands. The model predicted similar soil carbon stocks in the tundra to Post *et al*. (1982), but larger amounts of carbon in northern forest soils (Table 3). The total amount of carbon in present-day northern vegetation was predicted to be about 155 Pg, about 82% of which was in forests, divided about equally between coniferous and temperate/mixed forests (Table 3).

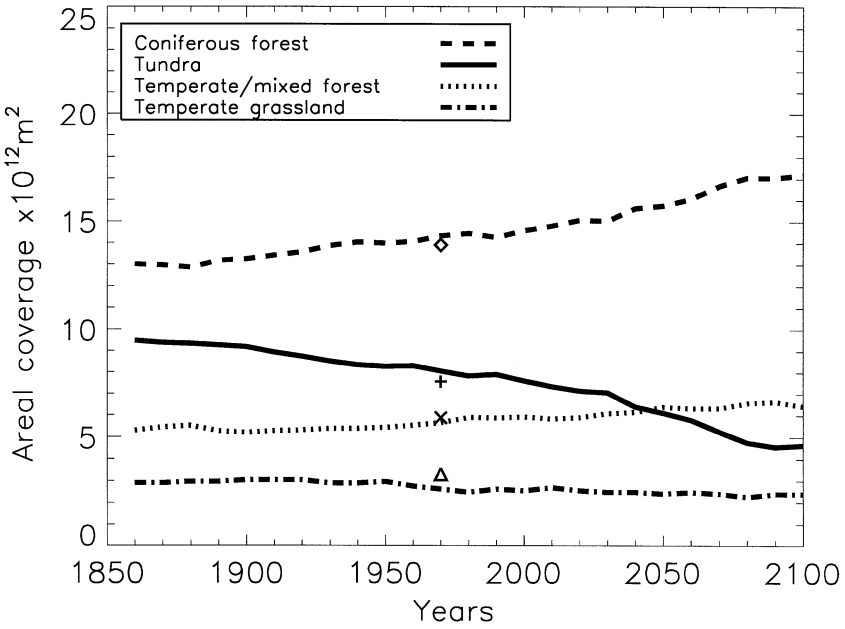

Fig. 3 Predicted changes in areas of four vegetation types in regions north of 50°N from 1860 to 2100 in response to transient climate change and increasing atmospheric CO_2 (IS92a). Also shown are the observational land cover estimates in 1970 taken from Matthews (1983), where ◇; is coniferous forest, + is tundra, × is temperate/mixed forest and △; is temperate grassland.

Changes in area of vegetation types over the period 1860–2100 in the absence of fire

During the period 1860–2100, the model predicted that climate change, combined with increased [CO_2] and N deposition, increased the area of coniferous plus temperate/mixed forest by about 50% ($15.5–23.5 \times 10^{12}$ m^2), mainly at the expense of tundra (Fig. 3). In 1860, the area north of 50°N was divided between tundra, coniferous forest, temperate/mixed forest and temperate grassland in the proportions 0.31, 0.42, 0.17, 0.10, whereas in 2100 the proportions were 0.15, 0.56, 0.21, 0.08, respectively. The original area of 9.5×10^{12} m^2 of tundra in 1980 was reduced to about 4.6x 10^{12} m^2 by 2100.

It is stressed that these model runs predicted *potential* vegetation cover, with no anthropogenic land-use change nor disturbance by fire or insects. The changes in vegetation distribution came about as a result of competition between the hybrid generalized plant types for environmental resources, assuming no dispersal constraints. The expansion of the forests occurred as a result of direct CO_2 and warming effects on tree photosynthesis and growth, and indirect effects due to increased soil N mineralization and improved water relations, particularly as a result of the increase in depth of unfrozen soil in the tundra.

Changes in total carbon stocks, NPP and potential NEP for all areas north of 50°N in the absence of fire

Figure 4 presents predicted totals, for all areas north of 50°N, in the store of carbon in soils and vegetation, in net primary productivity (NPP) and total soil or heterotrophic respiration, and in the resulting net ecosystem productivity (NEP) in the absence of fire. Predictions are shown with and without [CO_2] increasing, in both cases with N deposition increasing. Inter-annual variability, created by the daily weather generator, has been smoothed by taking the decadal mean of annual fluxes.

With both HadCM2 transient climate change (IS92a scenario) and CO_2 increasing, the model predicted an overall continuous increase in carbon in northern ecosystems from 1860 to 2100, totalling 134 Pg. Most of the increase occurred after about 1960 and all of it occurred in vegetation (Fig. 4a(i)). The soil carbon pool remained approximately constant until about 2000 and then lost about 23 Pg by 2100. Total regional annual NPP and soil (heterotrophic) respiration approximately doubled during the simulation, from about 15–30 PgC y^{-1} (Fig. 4a(ii)). The time trajectory of these increases closely followed those of temperature and [CO_2] (Fig. 1). From about 1900 onwards, there were many years when NPP exceeded soil respiration, giving a positive NEP — a carbon sink. This potential northern terrestrial sink (in the absence of fire) increased to a decadal average of about 0.46 PgC y^{-1} at the present time and to about 1.1PgC y^{-1} between 2050 and 2100 (Fig. 4a(iii)). The sink stabilized during the second half of the 21st century, as a result of accelerating rates of soil respiration and losses in soil carbon, despite continuously increasing NPP. However, there was little indication of a turndown in NEP up to 2100. It should be stressed that Fig. 4 hides large interannual variability. In any year, it was possible for regions to be a source or sink of carbon, depending on the simulated temperature and rainfall.

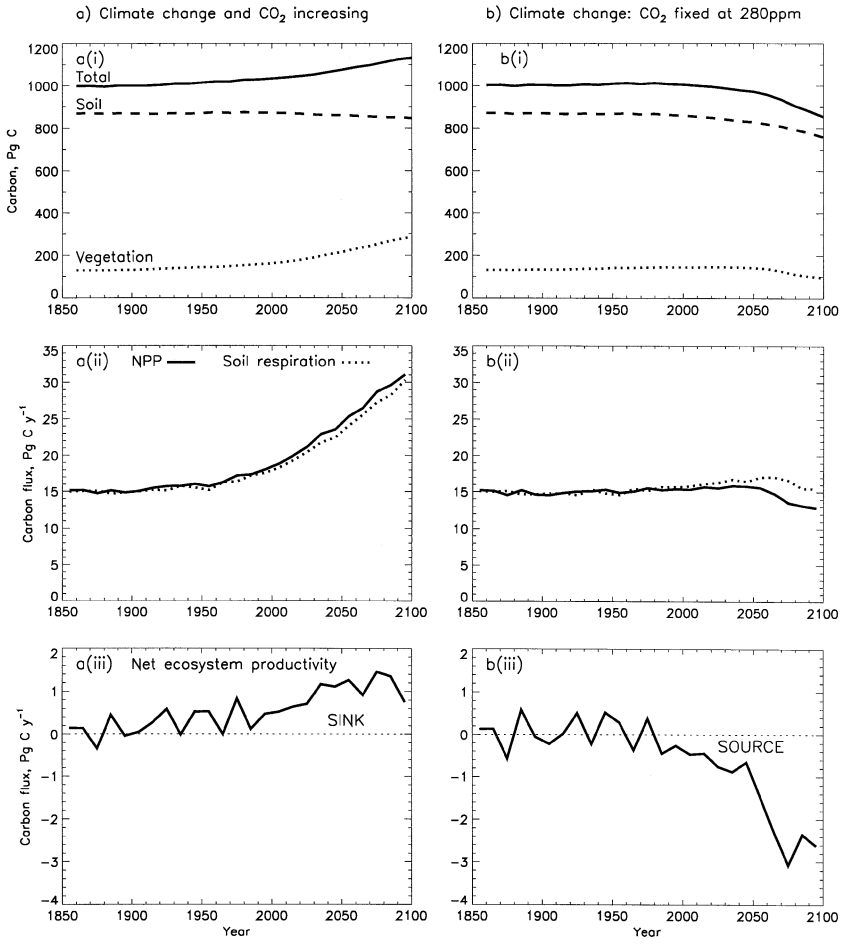

Fig. 4 Predicted changes in the total carbon pools (all vegetation and all soil) and mean carbon fluxes (net primary production, soil respiration and the difference, net ecosystem production) for all land areas north of 50°N in response to transient climate change (IS92a scenario) with and without increasing atmospheric CO_2. Large interannual variability has been smoothed by taking decadal mean values.

With HadCM2 transient climate change and N deposition alone ([CO_2] fixed at the 1860 value of 280 ppm), the model predicted loss of carbon in both vegetation and soils during the second half of the 21st century (Fig. 4(i)). Until about 1980, NPP and soil respiration increased only slightly above their 1860 values and remained approximately in balance. Thereafter, soil respiration exceeded NPP, and after 2050, NPP deceased, followed by decreased soil respiration as litter input to the soil carbon pool became smaller. The net result was a decrease in NEP, representing a carbon source of about 0.2 PgC y^{-1} at the present time, increasing to 2–3 PgC y^{-1} by the end of the next century (Fig. 4b(iii)). Thus, warming increased precipitation and N deposition alone did not create a carbon sink in northern terrestrial ecosystems; the sink was dependent upon the increase in NPP as a result of elevated [CO_2].

Effects of increased N deposition on carbon storage in the absence of fire

Predicted increases in atmospheric N deposition ranged from under 5 kgN ha^{-1} y^{-1} to over 40 kgN ha^{-1} y^{-1} in different regions (Fig. 2a), while biological N_2 fixation was set at 10 kg ha^{-1} y^{-1} for all model runs. Table 4 shows the effects of N deposition, determined by fixing deposition at 1860 values and taking 30-year mean values of NEP in order to smooth year-to-year variation. It is seen that N deposition was responsible for only 2% of the increase in NEP predicted for the whole region in the 30-year period centred on the 1990s and about 18% for the 2080s.

However, in areas of Europe which were predicted to receive over 20 kgN ha^{-1} y^{-1} by 2100 (Fig. 2a) N deposition was predicted to be responsible for about 5% of the increase in NEP in the 1990s increasing to around 34% by the 2080s (Table 4).

Changes in the geographical distribution and amount of tree biomass in the absence of fire

In this study, the classification of northern ecosystems into tundra, coniferous forest, temperate/mixed forest and temperate grassland was based on the proportion of tree to herbaceous biomass occurring in each grid cell and whether the biomass consisted predominantly of

	(1) N deposition fixed at 1860 value	(2) Increasing N deposition	Difference [(2)–(1)] Abs	%
All areas				
1990s	0.47	0.48	0.01	2
2040s	0.90	0.99	0.09	9
2080s	1.02	1.24	0.22	18
High deposition areas				
1990s	0.084	0.088	0.004	5
2040s	0.181	0.162	0.019	11
2080s	0.098	0.148	0.050	34

Table 4 Predicted 30-y mean net ecosystem productivity (Pg C y^{-1}) with and without increasing nitrogen deposition for all areas north of 50°N and in areas with high nitrogen deposition (greater than 20 kg N $ha^{-1} y^{-1}$ by 2100)

trees with broadleaved or needleleaved foliage. As is always the case when classifying vegetation, the ecosystem boundaries were somewhat arbitrary, depending on the classification criteria used. Rather than present maps of the four ecosystem classes, it is more revealing to examine the distribution of biomass in the underlying basic generalized plant types which contained most of the biomass — the broadleaved and needleleaved trees.

Fig. 5 shows the simulated distributions of biomass carbon occurring in broadleaved and needleleaved trees in 1860 and the predicted increase in carbon in those trees between the 1860s and 2090s in response to climatic change, increasing [CO_2] and N deposition. Note that individual grid squares can contain both types of tree, representing mixed species forests.

The 1860 simulations (Fig. 5a(i) and (ii)) showed that the model predicted the distribution of broadleaved and needleleaved trees in northern regions in reasonable agreement with observations (e.g. Matthews 1983; Olson *et al*. 1983). The main regions containing broadleaved trees in Europe, the Far East and southern Canada were well-defined, and the southern and northern boundaries of needleleaved forests were simulated satisfactorily at this regional scale. Inevitably, the tree biomass in some individual grid squares was overestimated or underestimated because of model limitations (e.g. the omission of nutrients other than N, soil hydrology, soil acidity and vegetation disturbance) but overall the simulations were remarkably good, given that the occurrence of generalized functional types was determined entirely by the effects of climatic factors on underlying plant physiological processes.

Between the 1860s and 2090s, the model predicted a northward expansion of needleleaved trees in Alaska, Canada and Siberia (Fig. 5b(ii)) with the consequent loss of about 5×10^{12} m^2 of tundra (Fig. 3). There was also some expansion of needleleaved forests southwards in continental Asia as a result of increased precipitation. By comparison, the model predicted only a modest northward expansion in areas of broadleaved trees, primarily in Europe (Fig. 5b(i)).

By far the most important change occurring between the 1860s and 2090s was an increase in both needleleaved and broadleaved tree biomass in most areas which already possessed these tree types in the 1860s (Fig. 6b(i) and (ii)). Needleleaved tree biomass increased by 5–10 kgC m^{-2} in much of the existing boreal forest in Canada and broadleaved tree biomass increased by 10–20 kgC m^{-2} in some areas of eastern Russia where needleleaved biomass was predicted to decrease. It is stressed that these predictions refer to potential biomass, assuming no changes in land use or fire frequency. Nevertheless, they suggest that the increase in carbon storage in forests, which may be primarily responsible for the predicted carbon sink in northern regions (Fig. 4), is likely to result more from an increase in the biomass of existing forests than from an expansion in forest area (see below).

Changes in carbon stocks, NPP and potential NEP of individual vegetation types in the absence of fire

In order to further examine the importance of increases in NPP and NEP within vegetation types compared to increases associated with redistribution of vegetation types, we returned to the four original vegetation classes and partitioned regions into those in which no change in vegetation type occurred between 1980 and 2100 and those in which a change occurred. Thus, in addition to regions where the vegetation remained unchanged, four new vegetation classes were created, these being regions which were originally coniferous forest and changed to temperate/mixed forest, from temperate/mixed forest to coniferous forest, from tundra to forest, and from temperate grassland to forest.

Figure 6 shows changes in the amount of carbon in vegetation and soils in the eight vegetation classes, together with the time-course of changes in NEP. Note that the NEP values were very variable between years,

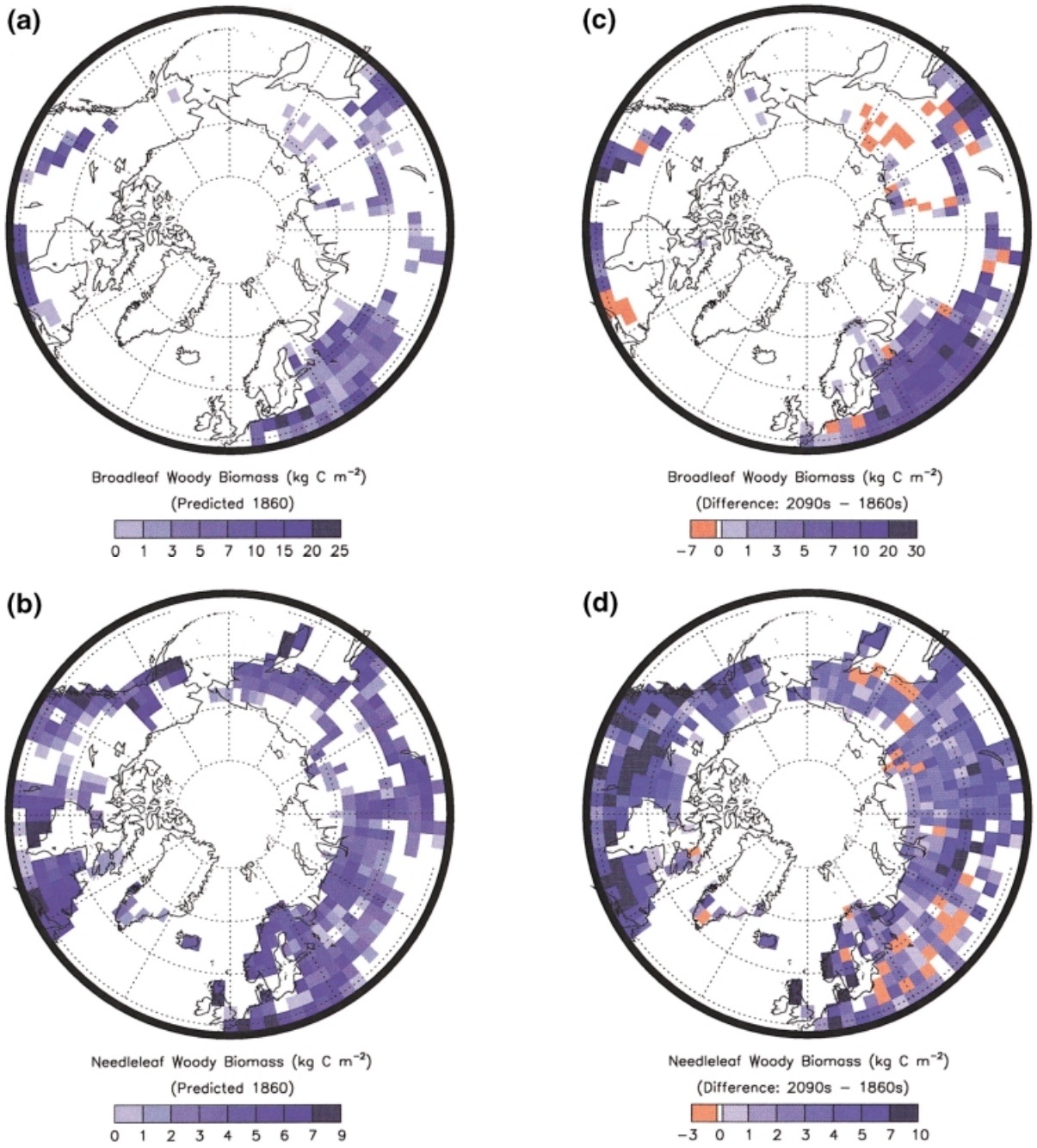

Fig. 5 Predicted biomass of broadleaved (a) and needleleaved (b) trees in 1860 and the change in broadleaved (c) and needleleaved (d) tree biomass between the 1860s and 2090s.

even when smoothed by taking decadal means. Table 5 presents mean NPP and NEP values for each vegetation class expressed per unit area as well as totalled for the area occupied by each class in the 1860s, 1990s and 2090s. Change was forced by climate, increased [CO_2] and N deposition.

The region-wide increase in carbon storage in vegetation, which was seen in Fig. 5, could be attributed overwhelmingly to increases in carbon storage in the biomass of areas which were already forest in 1860, and to a lesser extent to biomass that accumulated in tundra areas when they were converted to forest. Thus, carbon storage in both coniferous and temperate/mixed forests increased by 40 Pg between 1860 and 2100, while tundra areas which became forest during the simulation accumulated 20 Pg (Fig. 6a(i) and b(i)).

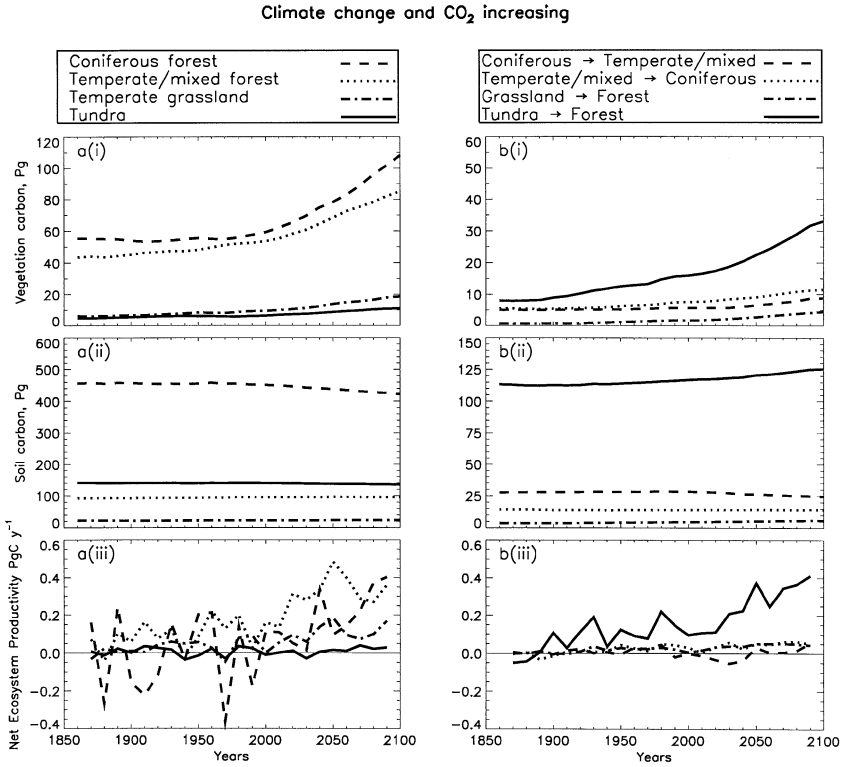

Fig. 6 Predicted changes in the carbon pools: (i) vegetation and (ii) soil) and (iii) mean net ecosystem productivity in areas north of 50°N, divided into areas where the four vegetation types did not change during the simulation (a, left) and where they changed, as shown (b, right) in response to transient climate change (IS92a scenario) with increasing atmospheric CO_2. Large interannual variability has been smoothed by taking decadal mean values.

Table 5 Predicted net primary productivity and net ecosystem productivity for 8 vegetation classes (4 classes when the vegetation type remains the same and 4 classes when the vegetation type changes during the simulation)

	1860s		1990s		2090s	
Productivity	tC $ha^{-1}y^{-1}$	Pg C y^{-1}	tC $ha^{-1}y^{-1}$	Pg C y^{-1}	tC $ha^{-1}y^{-1}$	tC $ha^{-1}y^{-1}$
Net primary (NPP)						
Coniferous forest	7.3	8.7	7.7	9.2	12.8	15.3
Temperate/mixed forest	7.6	3.6	8.7	4.1	13.3	6.2
Temperate grassland	2.0	0.4	3.0	0.7	5.3	1.2
Tundra	0.9	0.4	1.1	0.5	2.0	0.9
Coniferous–Temp/mixed forest	7.9	0.8	8.3	0.9	10.8	1.1
Temp/mixed–Coniferous forest	6.8	0.4	7.9	0.5	12.2	0.8
Temp grassland–Forest	1.1	0.1	3.2	0.2	8.0	0.5
Tundra–Forest	1.4	0.7	3.1	1.6	11.2	3.9
Net ecosystem (NEP)						
Coniferous forest	0.01	0.01	0.02	0.03	0.30	0.35
Temperate/mixed forest	0.02	0.01	0.27	0.13	0.68	0.32
Temperate grassland	0.00	0.00	0.25	0.06	0.48	0.11
Tundra	0.00	0.00	0.04	0.02	–0.02	–0.01
Coniferous–Temp/mixed forest	0.00	0.00	0.08	0.01	0.17	0.02
Temp/mixed–Coniferous forest	0.00	0.00	0.66	0.04	0.68	0.04
Temp grassland–Forest	0.00	0.00	0.30	0.02	0.72	0.05
Tundra–Forest	–0.08	–0.08	0.30	0.15	0.61	0.31

The small region-wide decrease in soil carbon, evident in Fig. 4, occurred mainly in coniferous forest areas, which were extensive, had carbon-rich soils (including peatlands) and occurred in northern regions which were subject to the greatest warming (Fig. 6a(ii)). There was little change in the amount of soil carbon in the other vegetation classes, except for tundra areas which became forest, which were the only areas to accumulate appreci-

Table 6 Predicted net ecosystem productivity with and without the effect of vegetation transition. Values without vegetation transition were estimated by scaling up the estimates from regions where transition did not occur

	(1) Without vegetation transition ($Pg\ C\ y^{-1}$)	(2) With vegetation transition ($Pg\ C\ y^{-1}$)	Difference [(2)–(1)]	
			Abs	%
1860s	0.02	–0.06	–0.08	–
1890s	0.01	0.02	0.01	–
1940s	0.24	0.36	0.12	33
1990s	0.29	0.46	0.17	37
2040s	0.73	1.00	0.27	27
2090s	0.86	1.19	0.33	28

able amounts of soil carbon (Fig. 6b(ii)). (Grasslands which become forest also accumulated soil carbon, but they were relatively small in area.)

Table 5 shows that all eight vegetation classes increased greatly in NPP between 1860 and 2100, the forests by 75%, temperate grassland by 165%, tundra by 122%, forest areas which changed from coniferous to temperate/mixed or *vice versa* by 25–35%, and the tundra and grassland areas which became forest by 600–700%.

These increases in NPP were responsible for increases in NEP in all vegetation classes except (i) coniferous forest areas in some years before 2000, when climatic variation caused carbon loss from the organic soils to exceed NPP, and (ii) tundra, where soil respiration exceeded NPP to produce a small carbon source by 2100. Tundra and grassland areas which became forest acquired NEP values per unit area similar to, or exceeding those, of existing forest. There was no evidence for a net loss of carbon when forests were transformed from one type to another (i.e. from forest dieback) although the NEP per unit area was small for areas converted from coniferous to temperate/mixed forest.

Overall, the potential carbon sink of $1.19\ Pg\ y^{-1}$ in the 2090 s in areas north of 50 °N could be attributed to carbon accumulation in coniferous forests (29%), temperate/mixed forests (27%), tundra which became forest (26%), temperate grassland (10%) and other vegetation classes (8%).

Quantitative effect of changes in distribution of vegetation types on potential NEP in the absence of fire

Quantitative estimates were made of the contribution made to the developing carbon sink during the period 1860–2100 by the redistribution of vegetation types — essentially the expansion of forest areas. That is, what would the sink size be if the areas of the forest areas had remained fixed? To achieve this, the NEP of each vegetation type which remained unchanged from 1860 to 2100 was scaled up to include areas in which transition occurred.

Table 6 shows that the sink of $1.19\ Pg\ y^{-1}$ in the 1990s would have been reduced by 28% to $0.86\ Pg\ y^{-1}$ had the vegetation types remained static. In fact, from the 1940s onwards, the expansion of the forest area was responsible for about 30% of the carbon sink.

Effect of boreal forest fires on carbon storage and NEP evaluated on plots in Quebec

Periodic forest fires, applied to needle-leaved forest plots in Quebec, reduced the average forest age and biomass, time-averaged NPP (because of reduced light interception over time), litter input to the soil and hence the amounts of soil carbon (Fig. 7). However, the NEP of the forest – the *increase* in biomass and soil carbon – was stimulated by climate change and increasing CO_2 (IS92a) during the period 1950–2100 equally as much with and without fire (Fig. 7d). Close examination showed that forest NEP was stimulated immediately after fire, because of the release of N in litter, despite N losses to the atmosphere.

However, when fires occur, the net exchange of carbon with the atmosphere is the NEP minus the carbon emitted during fires, which fluctuated from zero to 60 $gC\ m^{-2}\ y^{-1}$, taking decadal averages (Fig. 7b). This fire emission was 30–40% of the forest-soil NEP. For instance, over the period 2050–2100, fire emissions average 37 $gC\ m^{-2}\ y^{-1}$, while the NEP of forests with or without fire averaged about 120 $gC\ m^{-2}\ y^{-1}$. The net carbon exchange for the forest with fire was therefore about 83 $gC\ m^{-2}\ y^{-1}$ (120 minus 37), compared with 120 $gC\ m^{-2}\ y^{-1}$ without fire.

If coniferous forests represent 29% of the predicted northern latitude sink in 2050–2100 (see above) and fires reduce this sink by 30–40%, then the potential northern latitude sink of 1.19 $PgC\ y^{-1}$ would be reduced to 1.05 $PgC\ y^{-1}$. If all forest areas were affected by fire to the same extent (with an average return time of 167 years)

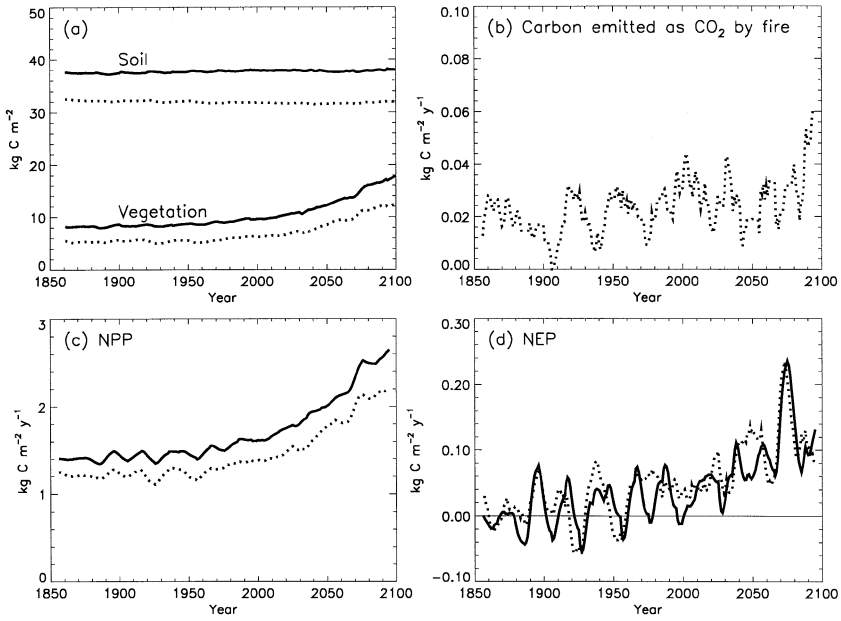

Fig. 7 Predicted effects of fire (dotted line), compared to without fire (solid line), on carbon pools and fluxes in an area of coniferous forest in southern Quebec. Here a fire return-time of 167 years (probability 0.006) is assumed. (a) Carbon storage in soils and vegetation. (b) Amount of carbon emitted in fires. (c) Net primary productivity. (d) Net ecosystem productivity. These are decadal averages with climate and CO_2 changing according to the IS92a scenario.

then the sink would be reduced to about 0.92 PgC y^{-1} in 2050–2100.

Discussion

This study used a combined biogeochemical, biophysical and biogeographical ecosystem model, with realistic transient behaviour (hybrid v4.1), driven by transient climate-anomaly output from a coupled atmosphere–ocean GCM (UK, Hadley Centre, Had CM2) and predicted atmospheric N deposition, to assess the current and future operation of the terrestrial carbon sink at latitudes above 50 °N resulting from business-as-usual radiative forcing from 1860 to 2100.

The study supports the conclusion that this region is currently a carbon sink, fluctuating annually about a mean of about 0.4 PgC y^{-1} (allowing for fire) and suggests that this sink could grow to about 0.8–1.0 PgC y^{-1} by 2100. Thus, the region, which covers about 25% of the vegetated global land area, may represent about 25–30% of the hypothesized current terrestrial carbon sink of about 1.6 PgC y^{-1} required to balance the current global carbon budget (Houghton *et al*. 1998). The remaining 1.2 PgC y^{-1} must be located in tropical and mid-latitudes. This study is in agreement with substantial evidence for a high-latitude carbon sink inferred from analyses of atmospheric CO_2 concentrations (see Introduction), observations of forest growth (see Introduction) and most other ecosystem modelling studies (Kohlmaier *et al*. 1995; Kellomäki & Vaisanen 1997; King *et al*. 1997; Cao & Woodward 1998b; Xiao *et al*. 1998). A study of Wang & Polglase (1995), based on the MAESTRO canopy model, is one of the few which predicts a high-latitude carbon source, apparently because, in this model, N limitations are not diminished by enhanced mineralization or greater N use efficiency in elevated [CO_2].

Most importantly, this study suggests that the high latitude sink is likely to persist until the end of the next century, despite greatly increased soil respiration in areas with up to 5–8 °C warming and progressive weakening of the CO_2-fertilization effect as [CO_2] increases to 800 ppm (Fig. 4). This conclusion is in agreement with other recent model studies (e.g. Cao & Woodward 1998b; Xiao *et al*. 1998), but we recognize that it rests on the assumption that photosynthesis will be stimulated substantially at elevated [CO_2] and temperature, that soil respiration will not overtake NPP as temperatures rise, and that severe nutrient limitations will not limit CO_2-fertilization (see Körner 1996).

In this discussion, we examine our assumptions concerning the responses of soil and plant respiration to temperature, the impact of fire and the three principal factors which produced the carbon sink in the model: (i) CO_2 enhancement of the NPP, NEP and biomass of existing forests (ii) amplification of this CO_2 enhancement by N deposition, and (iii) expansion of the forest area into former tundra and temperate grasslands.

Sensitivity to temperature dependence of soil and plant respiration

Predictions of the magnitude of the northern terrestrial carbon sink are thought to depend critically on the

temperature response functions chosen for soil organic matter decomposition (e.g. Anderson 1992; Kirschbaum 1995) and plant maintenance respiration, given the magnitude of warming depicted in Fig. 2(b). In this study, the temperature response functions were such that warming with no increase in [CO_2] substantially decreased soil organic matter and slightly decreased NPP after 2050 (Fig. 4b). With increasing [CO_2], these negative effects were overwhelmed by the predicted increase in NPP (Fig. 4a).

To test the sensitivity of these predictions, we varied both the temperature response functions for soil organic matter decomposition rate (equation 52 in Friend *et al*. 1997) and all maintenance respiration constants (equation 9 in Friend *et al*. 1997) by ± 20% and ran the model for the whole northern region with both climate change and [CO_2] increasing. In all runs, NEP followed the same increasing trend over time as shown in Fig. 4(a), with 50-y mean NEPs within 15% of the values in Fig. 4(a). This robustness may be attributed to increased N release when soil decomposition is accelerated and to the dominant effect of increasing [CO_2] on NPP.

It may be noted that Liski *et al*. (1999) suggested that old, high-latitude soils decompose less readily in response to increased temperature than assumed in most models, such as hybrid, which take temperature dependencies from litter decomposition studies. Forest soils in Finland show an *increase* in carbon storage with increase in mean annual temperature. In that case, our estimates of the northern sink may be conservative.

Effects of fire

Fire has profound effects on northern forest ecosystems, altering the N cycle, water relations and energy exchange. It is possible that our simple analysis missed important processes. However, as a first approximation, this study suggested that fire diminishes the northern terrestrial carbon sink by an amount of carbon approximately equal to that emitted to the atmosphere during fires. This amount is much smaller than the increase in carbon storage in biomass and soils as a result of CO_2 and N fertilization — with a fire return-time in all needle-leaved forests of over 100 years. Thus, our preliminary conclusion is that although the current frequency of fire disturbance will lessen the size and growth of the northern terrestrial carbon sink, it will not prevent it from occurring.

It should be noted that estimates of the effects of N deposition on the carbon sink were made only in the absence of fire, and fire was assumed to have no effect on vegetation distributions.

CO_2 enhancement of the NPP, NEP and biomass of existing forests

In the model, about 56% of the carbon sink in the 2090s was created as a result of an increase in the biomass of forests which already existed at the start of the simulation (Fig. 6). There was no net forest dieback (cf. Smith & Shugart 1993). The increase in biomass occurred essentially because the increase in [CO_2], combined with warming, increased canopy photosynthesis and water-use efficiency (Farquhar & von Caemmerer 1982; Friend 1995) which increased the standing biomass. Forest NPP increased greatly (Table 5), with consequently greater litter input to the soil. Most importantly, the large soil carbon pools in boreal coniferous and temperate/mixed forests were not appreciably depleted (Fig. 6), indicating that increased litter inputs balanced increased losses by soil respiration, even though soil respiration increased greatly over the temperature range in these cold climates (Kirschbaum 1995).

The increase in forest biomass and NPP was not highly constrained by N supply, because of an increase in foliar C:N ratio in elevated CO_2, enhanced N mineralization in response to soil warming and a net transfer of N from the soil to trees. In this respect, our model agrees with most others which include N dynamics (e.g. Kellomäki & Vaisanen 1997; Xiao *et al*. 1998). It may be noted that there is evidence that the NPP and biomass of European and tropical forests has increased in recent decades (Spiecker *et al*. 1996; Phillips *et al*. 1998).

Coniferous forests fluctuated between being a sink and source before 2000 and the tundra and grassland areas did so throughout most of the simulation, in accordance with observations in recent years (Fig. 6; Oechel *et al*. 1993; McKane *et al*. 1997). In tundra and grassland ecosystems, greatly increased NPP did not consistently match increased soil respiration and there was obviously no capacity for herbaceous plants to build up a large standing biomass.

Amplification of CO_2 enhancement by N deposition

Atmospheric N deposition amplified the CO_2-fertilization effect in the model, increasing the carbon sink in the region by only 2% at present, concentrated mostly in western Europe, but by about 30% by the end of the next century (Table 4) when substantial areas of Asia also received over 10 kgN ha^{-1} y^{-1} (Fig. 2d).

The mechanisms by which N addition increases NPP are well known and were represented in the model, notably, increased canopy photosynthesis when foliar N concentrations were at suboptimal levels, an amplified CO_2 response of light-saturated photosynthesis (McGuire *et al*. 1995), increased leaf area and lower C:N litter with

faster N mineralization. The growth of the model forests, like most boreal and temperate forests (Binkley & Högberg 1997; Reich *et al*. 1997) was positively related to annual soil mineral N supply, which was enhanced by N deposition as well as soil warming. A study using the hybrid model suggested that the NPP of conifer forests in Scotland may have been increased by 7–14% in recent decades by N deposition and 20–40% by the combination of N deposition, elevated CO_2 and warming (Cannell *et al*. 1998).

Most authors agree that N deposition is making a contribution to the global carbon sink, but estimates range from less than 0.2–1.3 PgC y^{-1} (Hudson *et al*. 1994; Townsend *et al*. 1996; Holland *et al*. 1997; McGuire *et al*. 1997; Nadelhoffer *et al*. 1999). The size of the N-fertilization effect depends on the fraction of deposited N that is retained in the system and the C:N ratio of the organic matter that accumulates. In this model, immobilization and leaching were represented, so that less than 50% of the N that was deposited was available for plant uptake in most regions and years. Our estimate of the N fertilization sink therefore falls midway between the controversial views of Schindler & Bayley (1993) that N deposition is the main driver of the northern terrestrial carbon sink and Nadelhoffer *et al*. (1999) that most deposited N is immobilized in low C:N soil organic matter.

Expansion of the forest area into former tundra and temperate grasslands

Unlike most previous models, including all those reviewed in the 1995 IPCC report (Kirschbaum *et al*. 1996) and all VEMAP models (Schimel *et al*. 1997), hybrid simulated dynamic shifts from one vegetation type to another, resulting from annual competition for light, N and water. In general, trees tended gradually to replace herbaceous plants wherever water and N became more available, combined with a general increase in water-use efficiency. Needleleaved trees encroached on the tundra in response to warming, which increased N mineralization and the depth and period of thawing, and forests expanded southwards in some areas, partly because of greater rainfall (Figs 2 and 5). These predictions are in broad agreement with comparable recent modelling studies (e.g. Cao & Woodward 1998b; Neilson & Draper 1998).

The rate of forest expansion was less than that predicted by 'climate envelope' models. However, the model assumed no constraints due to seed dispersal, anoxia, pH or disturbance, which can all be important in determining the tundra–boreal boundary (e.g. Crawford 1992; Starfield & Chapin 1996; Walker *et al*. 1998). Thus, in some areas forests moved several hundreds of kilometres within 100 years (over 1 km per year), which is at the upper end of postglacial forest migration rates (Ritchie & MacDonald 1986; Gear & Huntley 1991). Consequently, the carbon sink attributed to forest expansion should probably be regarded as an upper estimate (Table 6).

Nevertheless, this study suggests that the expansion of the northern forests could be large enough to modify current climate predictions by affecting both the carbon cycle and amplifying the climate feedbacks due to changes in surface albedo (Neilson & Draper 1998).

Conclusion

The hybrid model predicts that increasing [CO_2] and business-as-usual transient climate change predicted by the UK Hadley Centre GCM are increasing the NPP, biomass and NEP of forests at high latitudes, creating a carbon sink. This sink may be about 0.4 PgC y^{-1} at present, largely due to an increase in forest biomass and taking into account the carbon losses due to fire. Continued CO_2-fertilization and warming are predicted to sustain this sink over the next 100 years, but the extent to which it grows depends on the magnitude of N-fertilization and forest area expansion, which could potentially increase the sink to 0.8–1.0 PgC y^{-1}.

Acknowledgements

We are grateful to Deena Mobbs for assistance. This work was funded by the UK Department of Environment, Transport and Regions under contract number EPG 1/1/64 and by the EU ETEMA project.

References

Anderson JM (1992) Responses of soils to climate change. *Advances in Ecological Research*, **22,** 163–210.

Binkley D, Högberg P (1997) Does atmospheric deposition of nitrogen threaten Swedish forests? *Forest Ecology and Management*, **92,** 119–152.

Braswell BH, Schimel DS, Linder E, Moore B (1997) The response of global terrestrial ecosystems to inter-annual temperature variability. *Science*, **278,** 870–872.

Briffa KR, Schweingruber FH, Jones PD *et al.* (1998) Trees tell of past climates: but are they speaking less clearly today? *Philosophical Transactions of the Royal Society (London) B*, **353,** 65–73.

Cannell MGR, Thornley JHM, Mobbs DC, Friend AD (1998) UK conifer forests may be growing faster in response to increased N deposition, atmospheric CO_2 and temperature. *Forestry*, **71,** 277–296.

Cao M, Woodward FI (1998a) Net primary and ecosystem production and carbon stocks of terrestrial ecosystems and their responses to climate change. *Global Change Biology*, **4,** 185–198.

Cao M, Woodward FI (1998b) Dynamic responses of terrestrial

ecosystem carbon cycling to global climate change. *Nature*, **393,** 249–252.

Ciais P, Tans PP, Trolier M, White JWC, Francey RJ (1995) A large northern hemisphere terrestrial CO_2 sink indicated by the $^{13}C/^{12}C$ ratio of atmospheric CO_2. *Science*, **296,** 1098–1101.

Collatz GJ, Ball JT, Grivet C, Berry JA (1991) Physiological and environmental regulation of stomatal conductance, photosynthesis and transpiration: a model that includes a laminar boundary layer. *Agricultural and Forest Meteorology*, **54,** 107–136.

Comins HN, McMurtrie RE (1993) Long-term response of nutrient-limited forests to CO_2 enrichment. *Ecological Applications*, **3,** 666–682.

Conway TJ, Tans PP, Waterman LS, Thoning KW, Kitzis DR, Masarie KA, Zhang N (1994) Evidence for interannual variability of the carbon cycle from the National Oceanic and Atmospheric/Climate Monitoring and Diagnostics Laboratory global air sampling network. *Journal of Geophysical Research*, **99,** 22,831–22,855.

Crawford RMM (1992) Oxygen availability as an ecological limit to plant distribution. *Advances in Ecological Research*, **23,** 93–175.

Denning AS, Fung IY, Randall D (1995) Latitudinal gradient of atmospheric CO_2 due to seasonal exchange with land biota. *Nature*, **376,** 240–243.

Dixon RK, Brown S, Houghton RA, Solomon AM, Trexler MC, Wisniewski J (1994) Carbon pools and flux of global ecosystems. *Science*, **263,** 185–190.

Enting IG, Trudinger CM, Francy RJ (1995) A synthesis inversion of the concentration and d13C of atmospheric CO_2. *Tellus* B, **47,** 35–52.

Fan S, Gloor M, Mahlman J, Pacala S, Sarmiento J, Takahashi T, Tans P (1998) A large terrestrial carbon sink in North America implied by atmospheric and oceanic carbon dioxide data and models. *Science*, **282,** 442–446.

Farquhar GD, von Caemmerer S (1982) Modelling of photosynthetic response to environmental conditions. In: *Physiological Plant Ecology II. Water Relations and Carbon Assimilation* (eds Lange O *et al.*), Vol. 12B, pp. 549–587. Springer, Berlin.

Foley JA, Prentice CI, Ramankutty N, Levis S, Pollard D, Sitch S, Haxeltine A (1996) An integrated biosphere model of land-surface processes, terrestrial carbon balance and vegetation dynamics. *Global Biogeochemical Cycles*, **10,** 603–628.

Friend AD (1995) PGEN: an integrated model of leaf photosynthesis, transpiration and conductance. *Ecological Modelling*, **77,** 233–255.

Friend AD (1998) Parameterisation of a global daily weather generator for terrestrial ecosystem modelling. *Ecological Modelling*, **109,** 121–140.

Friend AD, White A (1999) Evaluation and analysis of a dynamic terrestrial ecosystem model under pre-industrial conditions at the global scale. *Global Biogeochemical Cycles*, in press.

Friend AD, Stevens AK, Knox RG, Cannell MGR (1997) A process-based. Biogeochemical, terrestrial biosphere model of ecosystem dynamics (Hybrid v3.0). *Ecological Modelling*, **95,** 249–287.

Gear AJ, Huntley B (1991) Rapid change in the range limits of Scots pine 4000 years ago. *Science*, **251,** 544–547.

Gorham E (1991) Northern peatlands: role in the carbon cycle and probable responses to climatic change. *Ecological Applications*, **1,** 182–195.

Goulden ML, Munger JW, Fan SM, Daube BC, Wofsy SC (1996) Exchange of carbon dioxide by a deciduous forest: response to inter-annual climate variability. *Science*, **271,** 1576–1578.

Goulden ML, Wofsy SC, Harden JW *et al.* (1998) Sensitivity of boreal forest carbon balance to soil thaw. *Science*, **279,** 2124–2217.

Holland EA, Braswell BH, Lamarque JF *et al.* (1997) Variations in the predicted spatial distribution of atmospheric nitrogen deposition and their impact on carbon uptake by terrestrial ecosystems. *Journal of Geophysical Research*, **102,** 15,849–15,866.

Houghton RA (1996) Terrestrial sources ans sinks of carbon inferred from terrestrial data. *Tellus B*, **48,** 420–432.

Houghton RA, Davidson EA, Woodwell GM (1998) Missing sinks, feedbacks and understanding the role of terrestrial ecosystems in the global carbon balance. *Global Biogeochemical Cycles*, **12,** 25–34.

Hudson RJM, Gherini SA, Goldstein RA (1994) Modeling the global carbon cycle: nitrogen fertilization of the terrestrial biosphere and the 'missing' sink. *Global Biogeochemical Cycles*, **8,** 307–333.

Hurtt G, Moorcroft PR, Pacala SW, Levin SA (1998) Terrestrial models and global change: challenges for the future. *Global Change Biology*, **4,** 581–590.

Jarvis PG (1976) The interpretation of the variation in leaf water potential and stomatal conductance found in canopies in the field. *Philosophical Transactions of the Royal Society (London) B*, **273,** 593–610.

Johns TC, Carnell RE, Crossley JF *et al.* (1997) The second Hadley Centre coupled ocean-atmosphere GCM: model description, spinup and validation. *Climate Dynamics*, **13,** 103–134.

Keeling CD, Whorf TP, Wahlen M, van der Pilcht J (1995) Interannual extremes in the rate of rise of atmospheric carbon dioxide since 1980. *Nature*, **375,** 666–670.

Keeling CD, Chin JFS, Whorf TP (1996) Increased activity of northern vegetation inferred from atmospheric CO2 measurements. *Nature*, **382,** 146–149.

Kellomäki S, Vaisanen H (1997) Modelling the dynamics of the forest ecosystem for climate change studies in the boreal conditions. *Ecological Modelling*, **97,** 121–140.

Kirschbaum MUF (1995) The temperature dependence of soil organic matter decomposition and the effect of global warming on soil organic carbon storage. *Soil Biology and Biochemistry*, **27,** 753–760.

Kirschbaum MUF, Fischlin A, Cannell MGR, Cruz RVO, Galinski W, Cramer WP (1996) Climate change impacts on forests. In: *Climate Change 1995. Impacts, Adaptations and Mitigation of Climate Change: Scientific-Technical Analyses. Working Party II of the Second Assessment Report of the IPCC* (eds Watson RT *et al.*), pp. 93–128. Cambridge University Press, Cambridge.

Kohlmaier GH, Hager Ch, Nadler A, Wurth G, Ludeke MKB (1995) Global carbon dynamics of higher latitude forests during an anticipated climate change: ecophysiological versus biome-migration view. *Water, Air and Soil Pollution*, **82,** 455–464.

King AW, Post WM, Wullschleger SD (1997) The potential response of terrestrial carbon storage to changes in climate and atmospheric CO_2. *Climatic Change*, **35,** 199–227.

Körner Ch (1996) The response of complex multispecies systems to elevated CO_2. In: *Global Change and Terrestrial Ecosystems*

(eds Walker B, Steffen W), pp. 20–42. Cambridge University Press, Cambridge.

Kurz WA, Apps MJ (1995) An analysis of carbon budgets of Canadian boreal forests. *Water, Air and Soil Pollution*, **82,** 321–331.

Liski J, Ilvesniemi H, Makela A, Westman CJ (1999) CO_2 emissions from soil in response to climatic warming are over-estimated – the decomposition of old soil organic matter is tolerant of temperature. *Ambio*, **28,** 171–174.

Matthews EJ (1983) Global vegetation and land-use: New high resolution data bases for climate studies. *Journal of Climate and Applied Meteorology*, **22,** 474–487.

McGuire AD, Melillo JM, Joyce LA (1995) The role of nitrogen in the response of forest net primary productivity to elevated carbon dioxide. *Annual Review of Ecology and Systematics*, **26,** 473–503.

McGuire AD, Melillo JM, Kicklighter DW *et al.* (1997) Equilibrium responses of global net primary production and carbon storage to doubled atmospheric carbon dioxide: sensitivity to changes in vegetation nitrogen concentration. *Global Biogeochemical Cycles*, **11,** 173–189.

McKane RB, Rastetter EB, Shaver GR, Nadelhoffer KJ, Giblin AE, Laundre JA, Chapin FS III (1997) Reconstruction and analysis of historical changes in carbon storage in Arctic tundra. *Ecology*, **78,** 1188–1198.

Mitchell JFB, John TC, Gregory JM, Tett SFB (1995) Climate response to increasing levels of greenhouse gases and sulphate aerosols. *Nature*, **376,** 501–504.

Monteith JL, Unsworth MH (1990) *Principles of Environmental Physics*. Edward Arnold, London.

Myneni RB, Keeling CD, Nemani RR (1997) Increased plant growth in the northern high latitudes from 1981 to 1991. *Nature*, **386,** 698.

Nadelhoffer KJ, Emmett BA, Gundersen P *et al.* (1999) Nitrogen deposition makes a minor contribution to carbon sequestration in temperate forests. *Nature*, **398,** 145–148.

Neilson RP, Running SW (1996) Global dynamic vegetation modelling: coupling biogeochemistry and biogeography models. In: Global change, terrestrial ecosystems (eds Walker B, Steffen W), pp. 451–465. Cambridge University Press, Cambridge.

Neilson RP, Draper RJ (1998) Potentially complex biosphere responses to transient global warming. *Global Change Biology*, **4,** 505–521.

Neilson RP, Prentice IC, Kittel T, Viner D (1998) Simulated changes in vegetation distribution under global warming. In: *The Regional Impacts of Climate Change: an Assessment of Vulnerability, a Special Report of IPCC WG II published for the Intergovernmental Panel on Climate Change* (eds Watson RT *et al.*), pp. 440–456. Cambridge University Press, Cambridge.

Oechel WC, Vourlitis GJ (1994) The effects of climate change on land-atmosphere feedbacks in arctic tundra regions. *Trends in Ecology and Evolution*, **9,** 324–329.

Oechel WC, Hastings SJ, Vourlitis G, Jenkins M, Riechers G, Grulke N (1993) Recent change of arctic tundra ecosystems from net carbon dioxide sink to source. *Nature*, **361,** 520–523.

Olson JS, Watts JA, Allison LJ (1983) *Carbon in Live Vegetation of Major World Ecosystems*, ORNL-5862, ESD Publications no. 1997. Oak Ridge National Laboratory, Oak Ridge, TN.

Parry ML, Carter TR, Hulme M (1996) What is a dangerous climate change? *Global Environmental Change*, **5,** 1–6.

Parton WJ, Scurlock JMO, Ojima DS *et al.* (1993) Observations and modelling of biomass and soil organic matter dynamics for the grassland biome worldwide. *Global Biogeochemical Cycles*, **7,** 785–809.

Phillips OL, Malhi Y, Higuchi N *et al.* (1998) Changes in the carbon balance of tropical forests: evidence from long-term plots. *Science*, **282,** 439–441.

Post WM, Emanuel WR, Zinke PJ, Stangenberger AG (1982) Soil Carbon pools and world life zones. *Nature*, **298,** 156–159.

Randerson JT, Thompson MV, Conmaw TJ, Fung IY, Field CB (1997) The contribution of terrestrial sources and sinks to trends in the seasonal cycle of atmospheric carbon dioxide. *Global Biogeochemical Cycles*, **11,** 535–560.

Reich PB, Grigal DF, Aber JD, Gower ST (1997) Nitrogen mineralization and productivity in 50 hardwood and conifer stands on diverse soils. *Ecology*, **78,** 335–347.

Richardson CW, Wright DA (1984) *WGEN: A model for generating daily weather variables*. U.S. Department of Agriculture, Agricultural Research Service, Temple, TX.

Ritchie JC, MacDonald GM (1986) The patterns of post-glacial spread of white spruce. *Journal of Biogeography*, **13,** 527–540.

Rolland C, Petitcolas V, Michalet R (1998) Changes in radial tree growth for *Picea abies*, *Larix decidua*, *Pinus cembra* and *Pinus uncinata* near the alpine timberline since 1750. *Trees*, **13,** 40–53.

Schimel DS, VEMAP participants, Braswell BH (1997) Continental scale variability in ecosystem processes: models, data and the role of disturbance. *Ecological Monographs.*, **67,** 251–271.

Schindler DW, Bayley SE (1993) The biosphere as an increasing sink for atmospheric carbon: estimates from increased nitrogen deposition. *Global Biogeochemical Cycles*, **7,** 717–733.

Smith TM, Shugart HH (1993) The transient response of terrestrial carbon storage to a perturbed climate. *Nature*, **361,** 523–526.

Spiecker H, Mielikainen K, Kohl M, Skovsgaard J (1996) Growth trends in European forests. *European Forest Research Institute Research Report No 5.* Springer, Heidelberg.

Starfield AM, Chapin IIFS (1996) Model of transient changes in Arctic and boreal vegetation in response to climate and land use change. *Ecological Applications*, **6,** 842–864.

Stewart JB (1988) Modelling surface conductance of pine forest. *Agricultural and Forest Meteorology*, **43,** 19–35.

Townsend AR, Braswell BH, Holland EA, Penner JE (1996) Spatial and temporal patterns in terrestrial carbon storage due to deposition of fossil fuel nitrogen. *Ecological Applications*, **6,** 806–814.

Walker DA, Auerbach NA *et al.* (1998) Energy and trace-gas fluxes across a soil pH boundary in the Arctic. *Nature*, **394,** 469–472.

Wang YP, Polglase PJ (1995) Carbon balance in the tundra, boreal forest and humid tropical forest during climate change: scaling up from leaf physiology and soil carbon dynamics. *Plant, Cell and Environment*, **18,** 1226–1244.

White A, Friend AF, Cannell MGR (1997) The impact of climate change on natural vegetation. In: *Climate Change and its Impacts: a Global Perspective.* UK Department of the Environment, Transport and Regions, UK Met. Office, Bracknell, 16pp.

Xiao X, Melillo JM, Kicklighter DW *et al.* (1998) Transient climate change and net ecosystem production of the terrestrial biosphere. *Global Biogeochemical Cycles*, **12,** 345–360.

Appendix

Soil temperature model within hybrid v4.1

A simple routine was developed to take into account differences in the depth of soil freezing (affecting decomposition, soil water availability and runoff) in order to improve the simulation of the forest–tundra boundary. Three soil layers were defined, 0–5 cm, 5–20 cm and 20–100 cm depth, and the temperature in each layer was derived from mean daily temperatures using second-order differential equations of heat conduction. We extend the description of Monteith & Unsworth (1990) and Wang & Polglase (1995) to simulate actual daily temperature values rather than assuming that temperature follows a sine wave distribution. If we assume that 24 h mean daily temperature can be represented by the function $f(t)$, and that the soil surface temperature equals $f(t)$ then

$$T_s(z,t) = T_a + \exp(-z/\xi)\,(f(t - t_d) - T_a),$$

where $T_s(z,t)$ represents the soil temperature at time t and depth z, T_a is the average annual temperature, t_d is the time delay for heat to be conducted to depth z, and $\xi = \sqrt{2\kappa/4}$, where κ is the thermal conductivity of the soil [assumed constant and parameterized as a clay soil, with a 0.2 liquid fraction, hence $\kappa = 0.046\ m^2\ day^{-1}$ (Monteith & Unsworth 1990)] and the angular frequency, $\omega = 2\pi/365\ day^{-1}$ for annual cycles. It can be shown that $t_d = z/\omega\zeta$ [by temporarily substituting $f(t)$ for a sine wave]. The depth at which frozen soil occurs can be found by setting equation 1 equal to zero.

It was assumed that herbaceous plants had access to water in the top two layers, whereas trees had access to all three layers. Whenever a soil water pool was below the frozen depth, all the water in that pool was considered frozen and therefore unavailable for uptake. When the frozen depth fell within a pool, only a fraction of the water within that pool was available. Whenever the soil was frozen, there was an additional constraint on the soil water potential seen by trees above that of herbaceous plants. That is, trees could access only a fraction, $0.5 + z_f/2$ (where z_f is the depth of frozen soil) of the water available to herbaceous plants (obviously, this fraction was restricted to be $\leqslant 1$). Decomposition was adjusted according to the fraction of unfrozen soil above 1 m in depth. The resistence to drainage from the third soil water pool was adjusted from 0.1 to 0.9 whenever the soil is frozen above 1 m.